Journal of Solid State Chemistry **148,** 135–142 (1999)
Article ID jssc.1999.8398, available online at http://www.idealibrary.com on IDEAL®

Quantum State Model of the Verwey Transition in Magnetite

H. Kloor[1] and J. M. Honig

Department of Chemistry, Purdue University, West Lafayette, Indiana 47907-1393

Received February 5, 1999; in revised form May 14, 1999; accepted May 24, 1999

DEDICATED TO PROFESSOR C. N. R. RAO, FRS, ON THE OCCASION OF HIS 65TH BIRTHDAY

Previous analyses of the Verwey transition in magnetite have been placed on a firm footing by a consistent analysis of the statistical properties of an array of quantum states associated with ferrous or ferric ions in octahedrally coordinated interstices of the spinel lattice. This collection is represented by an assembly of bonds and sites. Individual sites can be in one of three configurations: empty, as in the Fe^{3+} state, trapped, or polaronic if in the Fe^{2+} state. On neglect of high-energy states involving electron occupation of neighboring lattice sites, one arrives at an analytic equation of state for the order parameter in its dependence on temperature, which can be solved numerically. This equation is sufficiently flexible to handle both the first- and second-order transitions by appropriate changes in parameters. The present theory rationalizes the experimentally observed changes in the order of the Verwey transition that result from alterations in the sample stoichiometry. © 1999 Academic Press

1. BACKGROUND INFORMATION

The magnetite systems $Fe_{3(1-\delta)}O_4$, $Fe_{3-x}Zn_xO_4$, and $Fe_{3-y}Ti_yO_4$ (also designated as Verwey materials) pose an interesting theoretical challenge: it has been established through extensive experimentation (1) that with increasing δ, x, or y one encounters a change in the thermodynamic nature of the Verwey phase transformation. Namely, in the range $\delta \le \delta_c = 0.0039$ and for $x = y = 3\delta$ the transformation is first order, with a very sharp spike in the heat capacity anomaly and latent enthalpy at the Verwey transition temperature T_v; the corresponding entropy of transition is $\Delta S_v = R \ln 2$ at $\delta = 0$. Systems of this nature will be designated as belonging to class I. For $\delta_c \le \delta \le 3\delta_c$, as well as for $x = y = 3\delta$ in this range, the transition is of second order; a λ-like heat capacity anomaly is spread over a considerable temperature range about T_v, and no latent enthalpy of transition is encountered. The corresponding systems will be designated as belonging to class II. Finally, for $\delta > 3\delta_c$ and for $x = y = 3\delta$ the Verwey materials do not exhibit any low-temperature phase transitions; these compounds are classified as belonging to category III. The various manifestations of the above transformations (or lack thereof) will be collectively termed the Verwey transitions.

The limited aim of this introductory paper is to provide a unified approach for the theoretical description of the Verwey transitions. In later publications we intend to study in more detail the associated changes in thermodynamic and electrical transport properties.

The basic theory that can serve as a model for the study of Verwey transitions was outlined sometime ago by Straessler and Kittel (hereafter referred to as SK) in a brief paper (2) that deserves to be more widely known. More detailed accounts have recently been provided (3, 4). Basically, SK posited a ground state of energy $E_0 = 0$ with degeneracy g_0, occupied by n_0 out of N particles, and an excited state of energy $E \equiv E_1 = N[\varepsilon\psi - (1/2)\lambda\psi^2]$, with degeneracy g_1 and occupation $n_1 = N - n_0$. Here $\psi \equiv n_1/N$ may be considered as an order parameter; the $\varepsilon\psi$ and $-(1/2)\lambda\psi^2$ terms simulate, respectively, the degree of occupation of and the interaction between particles in the excited and ground state. The entropy is specified by $S = Nk_B \ln W$, with $W = g_0^{n_0} g_1^{n_1} N!/[(N-n_1)!\, n_1!]$, where k_B is the Boltzmann constant. On constructing the free energy via $F = E - TS$ and minimizing the latter with respect to ψ one obtains the *equation of state* characterizing equilibrium

$$\frac{\partial F}{\partial \psi} = 0 = \varepsilon - \lambda\psi - k_B T\left[\ln\frac{g_1}{g_0} + \ln\left(\frac{1-\psi}{\psi}\right)\right], \quad [1.1]$$

which must be solved numerically for $\psi(T; \Gamma)$, where the parameter set $\Gamma \equiv \lambda, \varepsilon, g_1/g_0$ must be specified. As SK demonstrated, the three choices $g_1/g_0 > 1$, $g_1/g_0 = 1$, or $g_1/g_0 < 1$ are sufficient to guarantee that $\psi(T, \Gamma)$ is discontinuous at a critical temperature T_v, that the first derivative is discontinuous at T_v, or that $\psi(T, \Gamma)$ remains continuous.

[1]To whom correspondence should be addressed. Present address: Entertaining Solutions, 10989 Bluffside Drive, Suite 3404, Studio City, CA 91604. E-mail: hkloor@aol.com.

0022-4596/99 $30.00

In other words, the SK equation of state is sufficiently flexible that first-order and second-order transitions (as well as no transitions) can be handled by the same formalism.

However, it is not obvious how the two-level approach can be correlated with the physical characteristics of Verwey materials. Rudimentary attempts to address this problem have been published (5). However, they suffer from shortcomings that have been detailed elsewhere (3). Here we construct a unified model that handles the Verwey transition problem without the inadequacies of the earlier work. The results are formally equivalent to the SK mean field approach. The present derivation is a variant of a more detailed version (3) to which the reader in referred for an alternative, more explicit exposition.

2. FUNDAMENTALS

It is well established that for temperatures $T_v > 121$ K Fe_3O_4 crystallizes as an inverse cubic spinel, with a unit cell comprised of 32 anions arranged on a face-centered cubic lattice; the cations fit into 8 out of 64 possible tetrahedrally coordinated interstices (c_4), and into 16 out of 32 octahedrally coordinated interstices (c_8). The former are known to be exclusively occupied by Fe^{3+} ions, while the latter contain Fe^{2+} and Fe^{3+} ions in equal concentration. Stated more accurately, the c_8 coordinated sites contain Fe^{3+} ion cores, with half as many "extra" electrons distributed among them. As a concomitant to the Verwey transition at $T_v < 121$ K the crystal suffers a slight distortion to the monoclinic structure; this transformation alters the degeneracies of the orbitals into which these extra electrons are placed. Incorporation of excess oxygen to form $Fe_{3(1-\delta)}O_4$ or doping with aliovalent Fe^{2+} and Ti^{4+} alters the density of the extra electrons.

The laws of mass conservation and electroneutrality can be used to deduce the actual cation distribution in nonstoichiometric magnetite of composition $Fe_{3(1-\delta)}O_4$. Assuming that the disorder occurs solely among c_8 sites the cation distribution is given by $(Fe^{3+})\,[Fe^{3+}_{1+6\delta}Fe^{2+}_{1-9\delta}\square_{3\delta}]\,O_4$ per formula unit (FU). Here (Fe^{3+}) represents trivalent iron occupying c_4 sites, while square brackets enclose cations Fe^{3+} and Fe^{2+} occupying c_8 sites; vacancies ($\square$) are generated when $\delta > 0$. For $\delta > 0$, $1 - 9\delta$ extra electrons are distributed among the $2 - 3\delta$ c_8 sites occupied by iron, and $1 + 6\delta$ sites remain vacant (note the distinction between vacant and unoccupied c_8 sites). The density of unoccupied sites C and of occupied sites D, respectively, is thus given by

$$C = (1 - 9\delta)/(2 - 3\delta) \approx \frac{1}{2} - \frac{15\delta}{4} = 1 - D \qquad [2.1]$$

$$D = (1 - 6\delta)/(2 - 3\delta) \approx \frac{1}{2} + \frac{15\delta}{4}. \qquad [2.2]$$

Since Ti^{4+} replaces iron exclusively in o-locations, $Fe_{3-y}Ti_yO_4$ must be represented by $(Fe^{3+})\,[Fe^{3+}_{1-2y}Fe^{2+}_{1+y}Ti^{4+}_y]\,O_4$, so that

$$C = \tfrac{1}{2}\,[1 + \tfrac{3}{2}\,y], \quad D = \tfrac{1}{2}[1 - \tfrac{3}{2}\,y] \quad \text{for } y \ll 1.$$

Zn^{2+}, on the other hand, replaces iron exclusively in t-locations so that $Fe_{3-x}Zn_xO_4$ is properly represented by $(Fe^{3+}_{1-x}Zn^{2+}_x)\,[Fe^{3+}_{1+x}Fe^{2+}_{1-x}]O_4$; this leads to $C = (1 - x)/2$, $D = (1 + x)/2$.

3. LATTICE REPRESENTATION

In our further development we now consider the extra electrons that are distributed among the octahedrally coordinated cations; we also restrict ourselves to undoped (though nonstoichiometric) magnetite. It is then reasonable to replace the entire magnetite lattice by the collection of c_8 coordinated cations and their associated extra electrons. The latter are placed into different types of states with their respective orbitals. Hence, the fundamental objects of the statistical analysis are considered to be these orbital states rather than the electrons that populate them. In a subsequent analysis we consider the degree of occupation of these orbitals by the extra electrons.

We now distinguish between the following configurations: (i) c_8 interstices populated by Fe^{3+} cores; these are designated as empty (e) states, accorded the symbol $\circ$ or X. The associated energies and degeneracies are ε_0 and λ_0, respectively. (ii) Trapped (t) states, which are generated when an electron resides at a c_8 site, subject to such a strong distortion of local surroundings that the charge carrier cannot acquire the necessary thermal energy to move to adjacent e states. The electron and distorted surroundings as a unit is assigned the symbol $\otimes$ or Y, an energy ε_1 and a degeneracy λ_1. (iii) Polaronic (p) states, wherein a given extra electron temporarily resides on a c_8 site, together with a slight distortion of the immediate anion surroundings. The resulting polaron can migrate as a unit to an adjacent e state, when thermal fluctuations temporarily bring the p and e states into energetic coincidence. This entity is assigned the symbol $\bullet$ or Z and is associated with energy ε_2 and degeneracy λ_2. The unit can acquire a directed drift (by hopping) under the influence of an applied electric field. These various configurations and their properties are summarized at the top of Table 1, together with the probabilities of their occurrence, α_i.

The above units cannot be considered in isolation. First, as already mentioned, a unit in the p state is capable of moving to an adjacent e state. Also, Coulomb interaction between electrons on adjacent c_8 sites affect the degree of occupation of the latter. We take these effects into account, but will ignore longer range interactions involving next-nearest neighbor c_8 sites. Even in the present approximation

TABLE 1

Designation	Figure	Energy	Degeneracy	Probability
X	○	ε_0	λ_0	α_0
Y	⊗	ε_1	λ_1	α_1
Z	●	ε_2	λ_2	α_2
XX	○—○	$\varepsilon_{0,0}$	$\lambda_{0,0}$	$\beta_{0,0}$
YY	⊗—⊗	$\varepsilon_{1,1}$	$\lambda_{1,1}$	$\beta_{1,1}$
ZZ	●—●	$\varepsilon_{2,2}$	$\lambda_{2,2}$	$\beta_{2,2}$
YZ	⊗—●	$\varepsilon_{1,2}$	$\lambda_{1,2}$	$\beta_{1,2}$
	●—⊗	$\varepsilon_{2,1}$		$\beta_{2,1}$
XZ	○—●	$\varepsilon_{0,2}$	$\lambda_{0,2}$	$\beta_{0,2}$
	●—○	$\varepsilon_{2,0}$		$\beta_{2,0}$
XY	○—⊗	$\varepsilon_{0,1}$	$\lambda_{0,1}$	$\beta_{0,1}$
	⊗—○	$\varepsilon_{1,0}$		$\beta_{1,0}$

Note. Definitions of the bond and site figure assemblies for the three state model. The type of state, figure representation, energy of the site or bond, degeneracy of the site or bond, and probability of occurrence is listed. It is assumed that $\varepsilon_{i,j} = \varepsilon_{j,i}$ and $\beta_{i,j} = \beta_{j,i}$.

the lattice itself is too complex a unit for statistical analysis. We therefore follow the approximation procedure of Hijmans and de Boer (5) in breaking down the lattice proper into assemblies of independent "bonds" (b) and "sites" (s) that form representative arrays. There are then nine distinct occupation states for the bonds that represent the various possible occupation states of neighboring c_8 lattice sites. These entities are listed in Table 1, along with their associated probabilities of occurrence, β_{ij}, energies, ε_{ij}, and degeneracies, λ_{ij}.

For a lattice where each site is surrounded by Z nearest neighbors we require $(Z/2)L$ bonds to represent all possible nearest neighbor pairs of c_8 sites. This b collection already includes ZL individual s sites, whereas the actual number of sites in the lattice proper is L. To compensate for the overcount we must therefore construct a site-figure s assembly of $(Z-1)L$ members whose energies and entropies are to be subtracted from the corresponding properties of the bond figure assembly.

4. STATISTICAL PROPERTIES

We begin the statistical treatment by referring to the listing of the possible occupation states in Table 1.

The energy of the bond b assembly is given by

$$U_b = \frac{Z}{2} L\left[\sum_{i=0}^{2} (\lambda_{0i}\beta_{0i}\varepsilon_{0i} + \lambda_{ii}\beta_{ii}\varepsilon_{ii}) - \lambda_{00}\beta_{00}\varepsilon_{00}\right], \quad [4.1]$$

where the last term compensates for the extra term in the summation that occurs when $i = 0$. The site s figure assembly that corrects for the site overcount in the b assembly has the energy

$$U_s = (Z-1)L\sum_{i=0}^{2} \lambda_i\alpha_i\varepsilon_i. \quad [4.2]$$

The entropy for g distinguishable configurations is specified by the Boltzmann expression $S = k_B\sum_g \lambda_g p_g \ln p_g$, where the p_g are the occupation probabilities. From Table 1 we obtain

$$S_b = -\frac{Z}{2} Lk_B\left[\sum_{i=0}^{2}\left(\lambda_{0i}\beta_{0i}\ln\beta_{0i} + \lambda_{ii}\beta_{ii}\ln\beta_{ii}\right) - \lambda_{00}\beta_{00}\ln\beta_{00}\right] \quad [4.3]$$

$$S_s = -(Z-1)Lk_B\sum_{i=0}^{2} \lambda_i\alpha_i\ln\alpha_i. \quad [4.4]$$

The total Helmholtz free energy per site pair $F = 2F/L$ is given by

$$\begin{aligned} F &= 2[(U_b - U_s) - T(S_b - S_s)]/L \\ &= Z\sum_{i=0}^{2}[\lambda_{0i}\beta_{0i}\varepsilon_{0i} + \lambda_{ii}\beta_{ii}\varepsilon_{ii} \\ &\quad + k_B T(\lambda_{0i}\beta_{0i}\ln\beta_{0i} + \lambda_{ii}\beta_{ii}\ln\beta_{ii}) \\ &\quad + 2(1/Z-1)(\lambda_i\alpha_i\varepsilon_i + k_B T\lambda_i\alpha_i\ln\alpha_i)] \\ &\quad - Z\lambda_{00}\beta_{00}(\varepsilon_{00} + k_B T\ln\beta_{00}). \end{aligned} \quad [4.5]$$

The nine variables β_{ij} and α_j are not all independent. First, the probabilities must be normalized to unity:

$$\sum_{i=0}^{2}(\lambda_{0i}\beta_{0i} + \lambda_{ii}\beta_{ii}) - \lambda_{00}\beta_{00} = 1 \quad [4.6]$$

$$\sum_{i=0}^{2}\lambda_i\alpha_i = 1. \quad [4.7]$$

Second, there exist consistency conditions which arise because the number of sites of type X in the bond and site figure assemblies of Table 1 must match the actual count, $\alpha_0 L$, in the lattice. When the multiplicities are properly taken into account we find that for sites of type X

$$(Z/2)L[2\lambda_{00}\beta_{00} + \lambda_{01}\beta_{01} + \lambda_{02}\beta_{02}] + (1-Z)L\lambda_0\alpha_0 = \alpha_0 L, \quad [4.8a]$$

or

$$2\lambda_{00}\beta_{00} + \lambda_{01}\beta_{01} + \lambda_{02}\beta_{02} = 2\lambda_0\alpha_0. \quad [4.8b]$$

Similarly, for sites of type Y or Z

$$2\lambda_{11}\beta_{11} + \lambda_{01}\beta_{01} + \lambda_{12}\beta_{12} = 2\lambda_1\alpha_1 \qquad [4.9]$$

$$2\lambda_{22}\beta_{22} + \lambda_{02}\beta_{02} + \lambda_{12}\beta_{12} = 2\lambda_2\alpha_2. \qquad [4.10]$$

Not all of these equations are unique. For if we sum [4.8b], [4.9], and [4.10] we obtain a form equivalent to [4.6], [4.7]. Thus, only four of the five above constraints are independent.

A final constraint arises from a match of compositions. The density of unoccupied sites which affects the actual electron density is specified by the experimental value of unoccupied c_8 sites in the lattice proper, C, as given by Eq. [3.1]

$$\lambda_0\alpha_0 = C. \qquad [4.11]$$

We arbitrarily consider Eq. [4.6] to be the redundant equation and select $\alpha_2, \beta_{22}, \beta_{02}, \beta_{00}$ as the independent variables. The dependent variables can then be specified as

$$\lambda_1\alpha_1 = 1 - \lambda_2\alpha_2 - C \qquad [4.12]$$

$$\lambda_{01}\beta_{01} = 2C - \lambda_{02}\beta_{02} - 2\lambda_{00}\beta_{00} \qquad [4.13]$$

$$\lambda_{12}\beta_{12} = 2\lambda_2\alpha_2 - \lambda_{02}\beta_{02} - 2\lambda_{22}\beta_{22} \qquad [4.14]$$

$$\lambda_{11}\beta_{11} = 1 + \lambda_{00}\beta_{00} + \lambda_{22}\beta_{22} + \lambda_{02}\beta_{02} - 2C - 2\lambda_2\alpha_2. \qquad [4.15]$$

We next enforce equilibrium by requiring $\partial F/\partial\beta_{00} = \partial F/\partial\beta_{02} = \partial F/\partial\beta_{22} = \partial F/\partial\alpha_2 = 0$ to minimize the free energy. The minimization process is straightforward but tedious. After a series of elementary steps detailed in Ref. (3) one finds the following interrelations among the occupation probabilities:

$$\ln(\beta_{00}\beta_{11}/\beta_{01}^2) = -E_1/k_BT \qquad [4.16a]$$

$$\ln(\beta_{02}\beta_{11}/\beta_{01}\beta_{12}) = -E_2/k_BT \qquad [4.16b]$$

$$\ln(\beta_{22}\beta_{11}/\beta_{12}^2) = -E_3/k_BT \qquad [4.16c]$$

$$\ln(\beta_{12}/\beta_{11}) + b\ln(\alpha_2/\alpha_1) = -(E_4 + E_d)/2k_BT, \qquad [4.16d]$$

wherein

$$b \equiv 1/Z - 1, \quad E_1 \equiv \varepsilon_{00} + \varepsilon_{11} - 2\varepsilon_{01},$$

$$E_2 \equiv (\varepsilon_{02} - \varepsilon_{01}) + (\varepsilon_{11} - \varepsilon_{12}),$$

$$E_3 \equiv \varepsilon_{22} + \varepsilon_{11} - 2\varepsilon_{12}, \quad E_4 \equiv (\varepsilon_{12} - \varepsilon_{11}) + 2b(\varepsilon_2 - \varepsilon_1)$$

$$E_d \equiv (\lambda_{00}/\lambda_2)\beta_{00}(\partial E_1/\partial\alpha_2) + (\lambda_{02}/\lambda_2)\beta_{02}(\partial E_2/\partial\alpha_2) + (\lambda_{22}/\lambda_2)\beta_{22}(\partial E_3/\partial\alpha_2) + \alpha_2(\partial E_4/\partial\alpha_2) + (1/\lambda_2)(\partial E_5/\partial\alpha_2) \qquad [4.17]$$

where

$$E_5 = C[2\varepsilon_{01} - \varepsilon_{11} + 2b(2\varepsilon_1 - \varepsilon_0)], \qquad [4.18]$$

Clearly, numerical solutions are required to specify the above β's and α's; moreover, six parameters are involved in the solution, not counting the individual energies nor the degeneracy factors in Eq. [4.17]. While brute force solutions can be obtained by numerical techniques they do not furnish systematic insight. A simpler approach is clearly desirable.

5. SIMPLIFICATION

Equations [4.16a]–[4.16d] become amenable to analytic formulations if we assume that the energy of all doubly occupied bonds is much greater than the energies of all other configurations. Such an assumption is not unreasonable, given the large coulombic repulsion between electrons located on nearest neighbor octahedral sites. Adoption of this assumption is equivalent to disallowing all double occupancies:

$$\beta_{11} = \beta_{12} = \beta_{22} = 0. \qquad [5.1]$$

This condition follows formally from the basic assumption, as shown elsewhere (3).

On introducing [5.1] into [4.11] to [4.15] and expanding [4.12] to first powers in δ ($\ll 1$) one obtains

$$2\lambda_0\alpha_0 = 2 - \Omega \qquad [5.2a]$$

$$2\lambda_1\alpha_1 = \Omega - \psi(T) \qquad [5.2b]$$

$$\lambda_{00}\beta_{00} = 1 - \Omega \qquad [5.2c]$$

$$\lambda_{01}\beta_{01} = 2\lambda_1\alpha_1 = \Omega - \psi(T) \qquad [5.2d]$$

$$\lambda_{02}\beta_{02} = 2\lambda_2\alpha_2 = \psi(T). \qquad [5.2e]$$

In the above we have introduced an order parameter ψ which is of intrinsic interest, and a stoichiometry parameter Ω, as

$$\psi \equiv 2\lambda_2\alpha_2, \qquad [5.3a]$$

$$\Omega \equiv 1 - 15\delta/2. \qquad [5.3b]$$

ψ will ultimately depend on T, due to the equilibrium constraints. Thus, the occupation variables are variously all specified in terms of T and δ.

6. ENERGY

With the above simplification the expression of the energy per pair of nearest neighbor sites reduces to

$$U = Z[\lambda_{00}\beta_{00}\varepsilon_{00} + \lambda_{01}\beta_{01}\varepsilon_{01} + \lambda_{02}\beta_{02}\varepsilon_{02}] + (1 - Z)[2\lambda_0\alpha_0\varepsilon_0 + 2\lambda_1\alpha_1\varepsilon_1 + 2\lambda_2\alpha_2\varepsilon_2]. \quad [6.1]$$

When Eqs. [5.2] and [5.3] are substituted and the results are simplified one obtains

$$U = Z(1 - \Omega)(\varepsilon_{00} - \varepsilon_0) + (2 - Z)\varepsilon_0 + Z(\Omega - \psi)\Delta_1(\psi) + Z\psi\Delta_2(\psi) + \psi G_2(\psi) - \Omega G_1(\psi), \quad [6.2]$$

where we have introduced four energy "gaps" as

$$G_2(\psi) \equiv \varepsilon_2 - \varepsilon_1 = G_2^0 + \psi G_2' \quad [6.3a]$$

$$G_1(\psi) \equiv \varepsilon_0 - \varepsilon_1 = G_1^0 + \psi G_1' \quad [6.3b]$$

$$\Delta_2(\psi) \equiv \varepsilon_{02} - \varepsilon_2 = \Delta_2^0 + \psi\Delta_2' \quad [6.3c]$$

$$\Delta_1(\psi) \equiv \varepsilon_{01} - \varepsilon_1 = \Delta_1^0 + \psi\Delta_1' \quad [6.3d]$$

In keeping with the methodology commonly used we have expanded each of the functions in [6.3] as a Taylor series in ψ, retaining only first-order terms. That is, we allow each gap to vary linearly with ψ, as shown on the right of Eqs. [6.3a]–[6.3d]. The superscripts 0 and the prime designate values of G_2 or G_1 and of its derivatives at $\psi = 0$. Next, substitute [6.3] into [6.2] and group the various coefficients of ψ^0, ψ, and ψ^2. On discarding the terms involving the constant parameters we obtain

$$U = [Z\Omega(\Delta_1' - G_1') + Z(\Delta_2^0 - \Delta_1^0) + G_2^0]\psi + [Z(\Delta_2' - \Delta_1') + G_2']\psi^2 \equiv m_0\psi - \tfrac{1}{2}m_1\psi^2. \quad [6.4]$$

Note that we have now arrived at the SK formulation for the energy of a two-level system. The constant value of the $\varepsilon_0 - \varepsilon_1$ gap, G_1^0, has been grouped with the discarded terms and has therefore disappeared. The leading term in ψ is given by $m_0 \sim G_2^0 \equiv \varepsilon_2^0 - \varepsilon_1^0$, while the remaining terms involve differences in gap energies and their derivatives, both of which are smaller. Likewise, the leading term in ψ^2 is given by $\frac{1}{2}m_1 \sim -G_2'$, just as in the SK theory. We have thereby obtained a physical interpretation of the parameters m_0 and m_1, (or ε and λ in the SK formulation) as applied to the Verwey problem.

7. THE ENTROPY

With the use of Eq. [5.1] we obtain the following expression for the entropy per pair of nearest neighbor sites:

$$-S/k_B = Z\{\lambda_{00}\beta_{00}\ln\beta_{00} + \lambda_{01}\beta_{01}\ln\beta_{01} + \lambda_{02}\beta_{02}\ln\beta_{02}\} + (1 - Z)\{2\lambda_0\alpha_0\ln\alpha_0 + 2\lambda_1\alpha_1\ln\alpha_1 + 2\lambda_2\alpha_2\ln\alpha_2\}. \quad [7.1]$$

On applying Eqs. [5.2] and [5.3] and carrying out the lengthy elementary algebraic manipulations we group the results into terms not involving ψ and terms involving ψ as

$$-S/k_B = Z\{(1-\Omega)\ln[(1-\Omega)/\lambda_{00}] - (2-\Omega)\ln[(2-\Omega)/2\lambda_0] + \Omega\ln(2\lambda_1/\lambda_{01})\} + (2 - \Omega)\ln[(2 - \Omega)/2\lambda_0] - \Omega\ln(2\lambda_1) + (\Omega - \psi)\ln(\Omega - \psi) + \psi\ln\psi + Z\psi\ln[\lambda_{01}\lambda_2/\lambda_{02}\lambda_1] + \psi\ln(\lambda_1/\lambda_2). \quad [7.2]$$

This result may be recast in the simple form

$$-S/k_B = (\Omega - \psi)\ln(\Omega - \psi) + \psi\ln\psi + \psi\ln(\psi_\otimes/\lambda_\bullet) + \ln r, \quad [7.3]$$

where $\ln r$ comprises all terms not involving ψ, and where

$$\lambda_\otimes \equiv (\lambda_{01}/\lambda_1)^Z\lambda_1 \quad [7.4a]$$

$$\lambda_\bullet \equiv (\lambda_{02}/\lambda_2)^Z\lambda_2. \quad [7.4b]$$

We relate λ_{01}, λ_{02}, λ_0, λ_1, λ_2 by writing

$$\lambda_{02}\beta_{02} = Q_2(\lambda_0\alpha_0)(\lambda_2\alpha_2) \quad [7.5a]$$

$$\lambda_{01}\beta_{01} = Q_1(\lambda_0\alpha_0)(\lambda_1\alpha_1) \quad [7.5b]$$

as two ways of specifying the probabilities of occupying XZ and XY site pairs; the Q_1, Q_2 are proportionality factors. On now inserting Eqs. [5.2] in [7.5] we obtain $Q_1 = Q_2 = 4/(2 - \Omega)$. In the mean field approximation that underlies the present theory we set $\beta_{0i} = \alpha_0\alpha_i$ $(i = 1, 2)$; we then obtain

$$\lambda_\otimes/\lambda_\bullet = \lambda_1/\lambda_2 \quad [7.6]$$

and

$$\ln r = (1 - \Omega)\ln\left(\frac{1 - \Omega}{\lambda_{00}}\right)^Z + (2 - \Omega)\ln\left(\frac{2 - \Omega}{2\lambda_0}\right)^{1-Z} + \Omega\ln(2\lambda_1)^{Z-1} - \Omega\ln\{[4/(2 - \Omega)]\lambda_0\lambda_1\}^Z. \quad [7.7a]$$

Of considerable interest is the case $\Omega = 1$, corresponding to stoichiometric magnetite. We find in place of [7.7a] the simple relation

$$\ln r = -\ln(4\lambda_0\lambda_1) = -\ln\lambda_{01}. \qquad [7.7b]$$

Thus, the entropy of stoichiometric magnetite at 0 K is governed solely by the degeneracy of the XY state.

8. THE FREE ENERGY MINIMIZATION

On assembling Eqs. [6.4] and [7.3] one may write the Helmholtz free energy per nearest neighbor site pair as

$$F = F(\psi; T, \delta) = m_0\psi - \tfrac{1}{2}m_1\psi^2 + k_BT[\ln r + \psi\ln\psi + (\Omega - \psi)\ln(\Omega - \psi) + \psi\ln(\lambda_\otimes/\lambda_\bullet)]. \qquad [8.1]$$

Finally, we enforce the equilibrium constraint $\partial F/\partial\psi = 0$, and set $\Omega = 1$, thereby ignoring effects arising from non-stoichiometry. This leads to the equation of state

$$\frac{m_0 - m_1\psi}{k_BT} = \ln\left(\frac{1-\psi}{\psi}\right) + \ln\left(\frac{\lambda_2}{\lambda_1}\right), \qquad [8.2]$$

which is of precisely the same SK form as Eq. [1.1].

9. DISCUSSION

As compared to the earlier attempts (5) the present approach provides a self-consistent connection between the experimental findings of the Verwey transition and the two-level SK theory. This unified theoretical development validates the data fitting procedures adopted previously (5) in the interpretation of the data along the lines of the SK theory.

To demonstrate the versatility of the theory we show in Figs. 1 and 2 the variation of the order parameter ψ with temperature T for a variety of $m_0/m_1 = \varepsilon/\lambda$ values. The functional dependence is found by numerical solution of the equation of state, Eq. [8.2] and is shown as a plot of ψ vs k_BT/λ. The physically realizable solutions are indicated by solid curves while the dotted curves show ranges of ψ that are not accessible. Figure 1a for $m_0/m_1 = \varepsilon/\lambda = 5/9$ clearly shows the discontinuity in the order parameter characteristic of a first-order transition. Note that beyond the transition temperature T_v, ψ diminishes with rising T, a feature which SK described as a super-transition. The variation of ψ with k_BT/λ for $m_0/m_1 = \varepsilon/\lambda = 2/3$ gives rise to a normal first-order transition, shown in Fig. 1b, wherein ψ continues to rise with $T > T_c$. Note the detailed diagram of Fig. 2 which shows the existence of loops that require a Maxwell construction with equal areas A and B, as shown in the figure; the dividing line defines the temperature T_v. Thus, the theory successfully models gradual changes in order parameter that terminate in a first-order transition at the critical temperature. Finally, we show in Fig. 1c the change of ψ with k_BT/λ for $m_0/m_1 = \varepsilon/\lambda = 0.5$, which is indicative of a second-order transformation, wherein ψ is continuous but its first derivative is discontinuous at T_c.

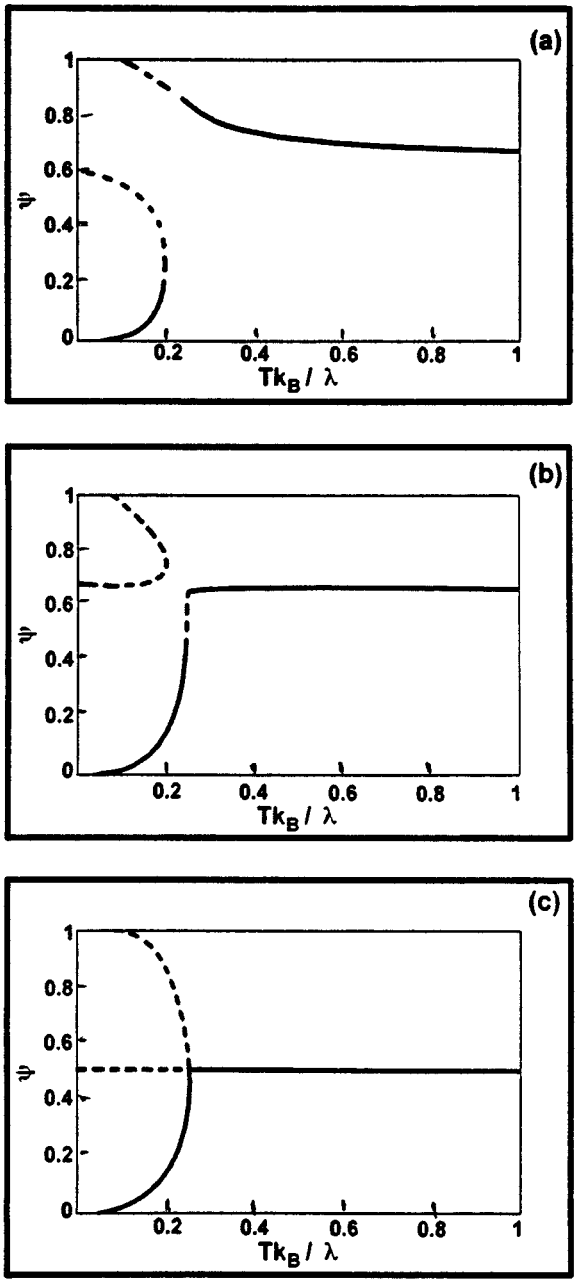

FIG. 1. Plot of order parameter ψ vs k_BT/λ for $\varepsilon/\lambda = 5/9$ (Part (a)), 2/3 (part (b)), 1/2 (part (c)), respectively. Here $\varepsilon \equiv m_0$, $\lambda \equiv m_1$. Dotted curves represent unphysical solutions.

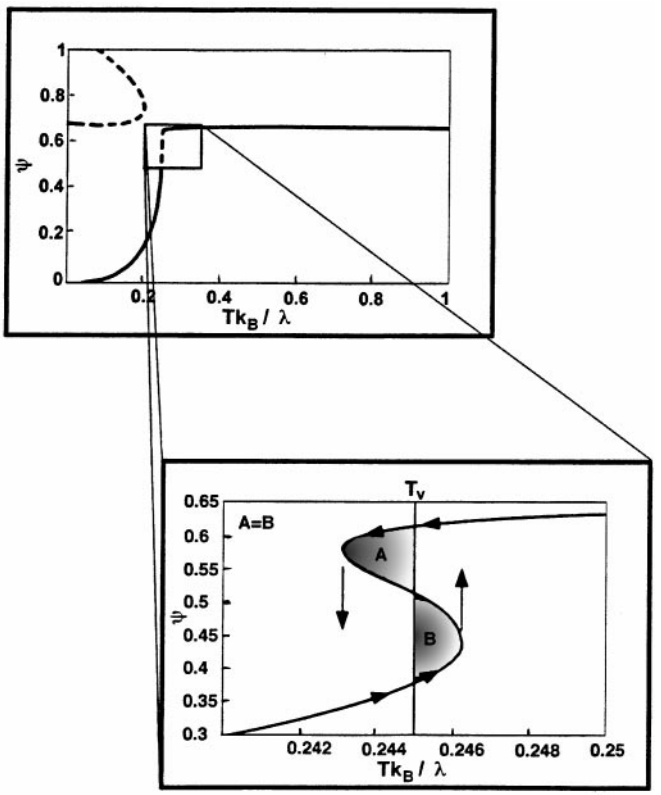

FIG. 2. Detailed representation of Fig. 1b. Insert shows discontinuity in the order parameter at $k_BT/\lambda = 0.245$, determined by a Maxwell construction that equalizes areas A and B inside the loops. Arrows indicate the hysteresis path.

We test the validity of the present theory by confrontation with experiment. Such tests were already undertaken earlier (5) with the SK model; thus, a brief review of the findings suffices. One needs to determine three parameters: m_0, m_1, and λ_2/λ_1 for use in Eq. [8.2]. We begin by taking the difference in entropy S_v just above and just below the Verwey transition temperature T_v, using Eqs. [7.3] and [7.6] with $\Omega = 1$ and set $\psi_1 \equiv \frac{1}{2}(1-\Delta), \psi_2 = \frac{1}{2}(1+\Delta)$ to find

$$S_v = N\Delta \ln(\lambda_2/\lambda_1). \qquad [9.1]$$

For stoichiometric magnetite the experimental value for the molar entropy of the Verwey transition is close to $R\ln 2$ (7); allowing for two octahedral sites per formula unit requires that we set $\Delta = \frac{1}{2}$ and $\lambda_2/\lambda_1 = 2$. The parametrizations for m_0 and m_1 were performed by noting how T_v varies with deviations from ideal stoichiometry (δ in $Fe_{3(1-\delta)}O_4$), as detailed elsewhere (5). One finds that

$$m_0(\delta) = k_B[3.862\, T_v(\delta) - 118.0] \qquad [9.2a]$$

$$m_1(\delta) = k_B[6.338\, T_v(\delta) - 236.1] \qquad [9.2b]$$

for first-order samples ($101.0 \le T_v \le 121.1$ K).

We now carry out three tests of the model using the above parametrization. (i) One can determine S_v as described earlier, but now allowing δ (and thereby, T_v) to vary. The resulting plot is shown in Fig. 3 as a continuous curve. The corresponding experimental values are superposed as points. The agreement is very satisfactory. (ii) Without changes in parameter one may determine the variation of the Seebeck coefficient α with temperature for a fixed composition. This requires the determination of the Fermi level ξ for use in the relationship $\alpha = \xi/eT$, on neglect of the kinetic energy contribution. From conservation of charge one may determine ξ through the relation (3,5)

$$\frac{1}{2} = \frac{\lambda_2\psi}{1+\exp(-\xi/k_BT)} \frac{\lambda_1(1-\psi)}{1+\exp\{[-(m_0-m_1\psi)-\xi]\}/k_BT}. \qquad [9.3]$$

With the indicated parametrizations, setting $\lambda_2 = 2\lambda_1 = 2$, $\delta = 0$, and determining ψ via Eqs. [8.2] and [9.2] one obtains ψ as a function of T, thence $\xi(T)$ from Eq. [9.3], and finally, $\alpha = \xi/eT$. The result is plotted in Fig. 4 as the full curve. The experimental results (8) are shown as a dashed curve. It must be remembered that no additional assumptions have been introduced. The agreement between theory and experimental is satisfactory. (iii) The electrical conductivity σ is given by $\sigma = ne\mu$, where

$$n = 2\lambda_2\psi/[1+\exp(-\xi/k_BT)] \qquad [9.4a]$$

is the mobile charge carrier density. The mobility is assumed to be specified by the small polaron model $\mu = (1-c)ea^2\Gamma/k_BT$, where

$$1 - c = \lambda_1(1-\psi)/\{[1+\exp[-(m_0-m_1\psi)-\xi]/k_BT]\} \qquad [9.4b]$$

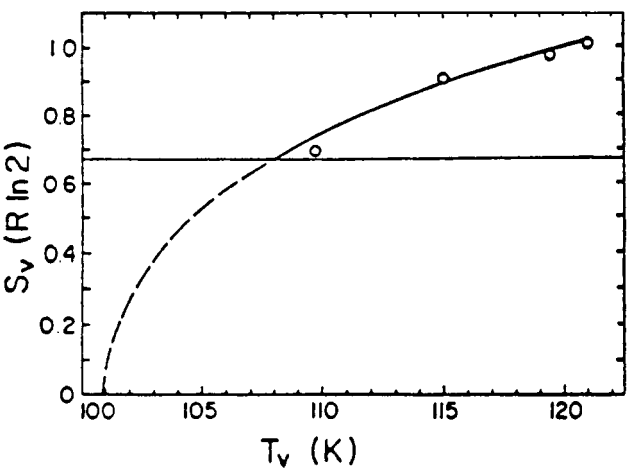

FIG. 3. Plot of calculated (full curve) vs experimentally observed entropy changes at the first-order Verwey transition in $Fe_{3(1-\delta)}O_4$. The transition temperature T_v shifts downward with increasing δ.

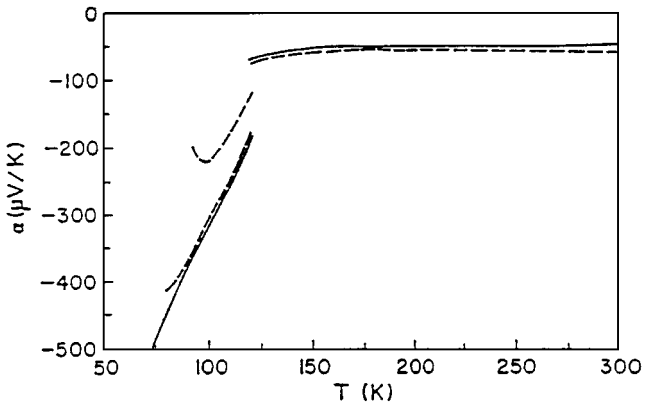

FIG. 4. Analysis of Seebeck coefficient $\alpha = \xi/eT$ for Fe_3O_4 (full curve), compared to experimental measurements (dashed curve). The upper dashed curve is measured for Fe_3O_4 containing slight impurities.

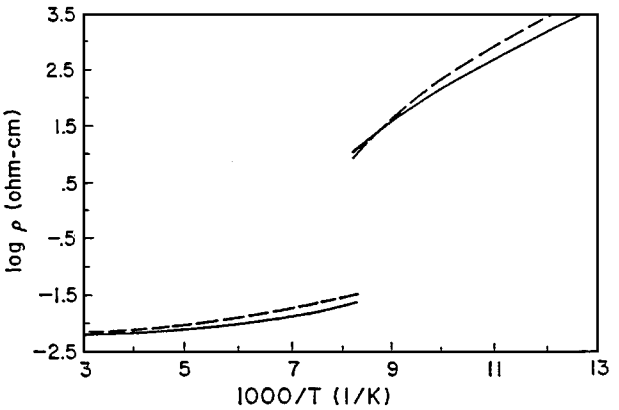

FIG. 5. Analysis of resistivity ρ as plot of $\log \rho$ vs $1/T$ for Fe_3O_4. The full curve is the calculated set of ρ values; the dashed curve represents experimental data. The theoretical parameters were fixed at the crossover points, but the remaining temperature variation of the full curve is determined by the theory.

is the fraction of octahedral sites devoid of the extra electrons and a is the separation distance between adjacent octahedral sites. Γ is the jump rate of the polaron, which in the limiting form, is given by

$$\Gamma = pv_0 \exp(-m_0/k_B T), \qquad [9.5]$$

where v_0 is the appropriate optical phonon frequency and p is the probability of encountering a jump during a coincidence event involving initial and final sites. The variation of the resistivity $\rho \equiv 1/\sigma$ was then determined as a function of T with $\delta = 0$. In these calculations pv_0 was treated as an adjustable parameter, determined by fitting it separately to experimetal results at a specific temperature in the range below and above T_v. The variation of ρ with T is then fully determined by the theory. In Fig. 5 we show plots of $\log \rho$ vs $1/T$: the full curve represents the theory, the dashed curve represents the experiments (8). Once again, the agreement is satisfactory.

In conclusion, we have provided a theoretical description of both thermodynamic and electrical transport properties of $Fe_{3(1-\delta)}O_4$ using a model related to order–disorder theory. As formulated above, this approach handles both the first- and second-order manifestations of the Verwey transition and satisfactorily accounts for a variety of experimental data pertaining to magnetite.

ACKNOWLEDGMENTS

This research was supported in part by NSF Grant 96-12130-DMR. Useful discussions with Drs. Jozef Spałek and Carrick Talmadge are gratefully acknowledged.

REFERENCES

1. For reviews see: J. M. Honig, *Proc. Indian Acad. Sci* (*Chem. Sci.*) **96,** 391 (1986); J. M. Honig, *Phys. Chem. Miner.* **15,** 476 (1988); J. M. Honig and J. Spałek, *in* "Solid State Physics-2" (M. A. K. L. Dissanayake, K. Tennakone, D. A. Ilemperuma, Eds.), p. 41. Nova Science, Commack, NY, 1991; M. Yethiraj and J. M. Honig, *in* "Advances in the Synthesis and Reactivity of Solids" (T. E. Mallouk, Ed.), Vol. 2, p. 235. JAI Press, London, 1994; J. M. Honig, *J. Alloys Compds.* **229,** 24 (1995).
2. S. Straessler and C. Kittel, *Phys. Rev.* **139,** A758 (1965).
3. H. Kloor, unpublished thesis, Purdue University, 1994.
4. J. M. Honig, *J. Chem. Ed.* **76,** 848 (1999).
5. R. Aragón and J. M. Honig, *Phys. Rev. B* **37,** 209 (1988); J. M. Honig, *Phys. Chem. Miner.* **15,** 476 (1988); J. M. Honig and R. Aragón, *Physica B* **150,** 129 (1988); J. M. Honig and P. Gopalan, *Solid State Ionics* **32–33,** 82 (1989); J. M. Honig, J. Spałek, *J. Less Common Metals* **156,** 423 (1989); J. M. Honig, J. Spałek, and P. Gopalan, *J. Am. Ceram. Soc.* **73,** 3225 (1990); J. M. Honig and J. Spałek, *J. Solid State Chem.* **96,** 115 (1992); J. M. Honig, *J. Alloys Compds.* **229,** 24 (1995).
6. J. Hijmans and J. de Boer, *Physica* **21,** 471, 485, 499 (1955).
7. J. P. Shepherd, J. W. Koenitzer, R. Aragón, C. J. Sandberg, and J. M. Honig, *Phys. Rev. B* **31,** 1107 (1985).
8. R. J. Rasmussen, R. Aragón, and J. M. Honig, *J. Appl. Phys.* **61,** 4395 (1987).